

Supporting Information:
Characterization of Carrier Cooling Bottleneck in Silicon Nanoparticles
by Extreme Ultraviolet (XUV) Transient Absorption Spectroscopy

Ilana J. Porter,^{†,‡,#} Angela Lee,^{†,@} Scott K. Cushing,^{†,‡,△} Hung-Tzu Chang,[†]
Justin C. Ondry,^{†,¶,▽} A. Paul Alivisatos,^{†,¶,§,||} and Stephen R. Leone^{*,†,‡,⊥}

[†]*Department of Chemistry, University of California, Berkeley, CA 94720, USA.*

[‡]*Chemical Sciences Division, Lawrence Berkeley National Laboratory, Berkeley, CA 94720, USA.*

[¶]*Kavli Energy NanoScience Institute, Berkeley, CA 94720, USA.*

[§]*Materials Sciences Division, Lawrence Berkeley National Laboratory, Berkeley, CA 94720, USA.*

^{||}*Department of Materials Science and Engineering, University of California, Berkeley, CA 94720, USA*

[⊥]*Department of Physics, University of California, Berkeley, CA 94720, USA.*

[#]*The authors contributed equally to this work.*

[@]*The authors contributed equally to this work. Current address: Department of Chemistry, Massachusetts Institute of Technology, Cambridge, MA 02139, USA.*

[△]*Current address: Division of Chemistry and Chemical Engineering, California Institute of Technology, Pasadena, CA, 91125, USA.*

[▽]*Current address: Department of Chemistry, James Franck Institute, and Pritzker School of Molecular Engineering, University of Chicago, Chicago, Illinois 60637, USA.*

E-mail: srl@berkeley.edu

Supplemental Methods

XPS

X-ray photoelectron spectroscopy measurements were performed at the Imaging and Manipulation of Nanostructures Facility of the Molecular Foundry at the Lawrence Berkeley Lab. Samples were produced by drop casting the nanoparticle in ethanol solution onto sonication-cleaned tantalum foil. Measurements of the silicon $2p$ peak were obtained using a K-Alpha Plus XPS/UPS with a spot size of $400\ \mu\text{m}$. An ion flood gun was used to minimize surface charging. Curve fitting was performed with Thermo ScientificTM Advantage Software.

TEM

TEM imaging was performed on a FEI Tecnai T20 S-TWIN TEM operating at 200kV with a LaB₆ filament. TEM images of the nanoparticle samples were collected with a Gatan Orius SC200 TEM camera with a 1 second exposure time. TEM images, selected area diffraction patterns, and dark field TEM images of the thin film sample were collected with a Gatan RIO16IS camera, with the dark field images collected by placing the objective aperture around the 004 diffraction peak. Nanoparticle samples were prepared by drop casting a solution of the particles onto a carbon coated copper TEM grid (CF400-CU). The density of nanoparticles on the TEM grid is lower than that used in the XUV measurements in order to resolve the individual nanoparticles. Thin film samples were prepared by breaking the thin film membrane into small pieces using a diamond scribe and gently pressing the TEM grid into the pieces.

Powder XRD

Powder diffraction patterns of the nanocrystalline samples were obtained using a Bruker D-8 GADDS diffractometer equipped with a Co $K\alpha$ source. XRD was collected in reflection geometry with an incident X-ray angle (ω) of 15° . 2D patterns were merged and integrated in

the DIFFRAC.EVA software from Bruker. The 1D diffraction patterns were then converted from 2θ to $q(\text{\AA}^{-1})$ to remove the X-ray wavelength dependence. Nanoparticle samples were prepared by drop casting a concentrated solution of nanocrystals on a low background $\langle 510 \rangle$ oriented silicon substrate.

Diffraction patterns of the Si(100) thin film were collected using a Bruker Phaser D2 diffractometer with Cu $K\alpha$ source operated at 30 kV and 10 mA with a 160 SSD detector. Low (high) resolution diffraction patterns were collected from 25° to 75° 2θ (68° to 71° 2θ) with a step size of 0.04° (0.01°) and an integration time of 5s (3s) per step. Contribution from the $K\alpha_2$ diffraction was removed using the DIFFRAC.EVA software. Thin film samples were prepared by placing a silicon thin film membrane face down on a $\langle 510 \rangle$ oriented low background silicon substrate and gently pressing the corners with a diamond scribe to release it from the support frame.

Supplemental Figures

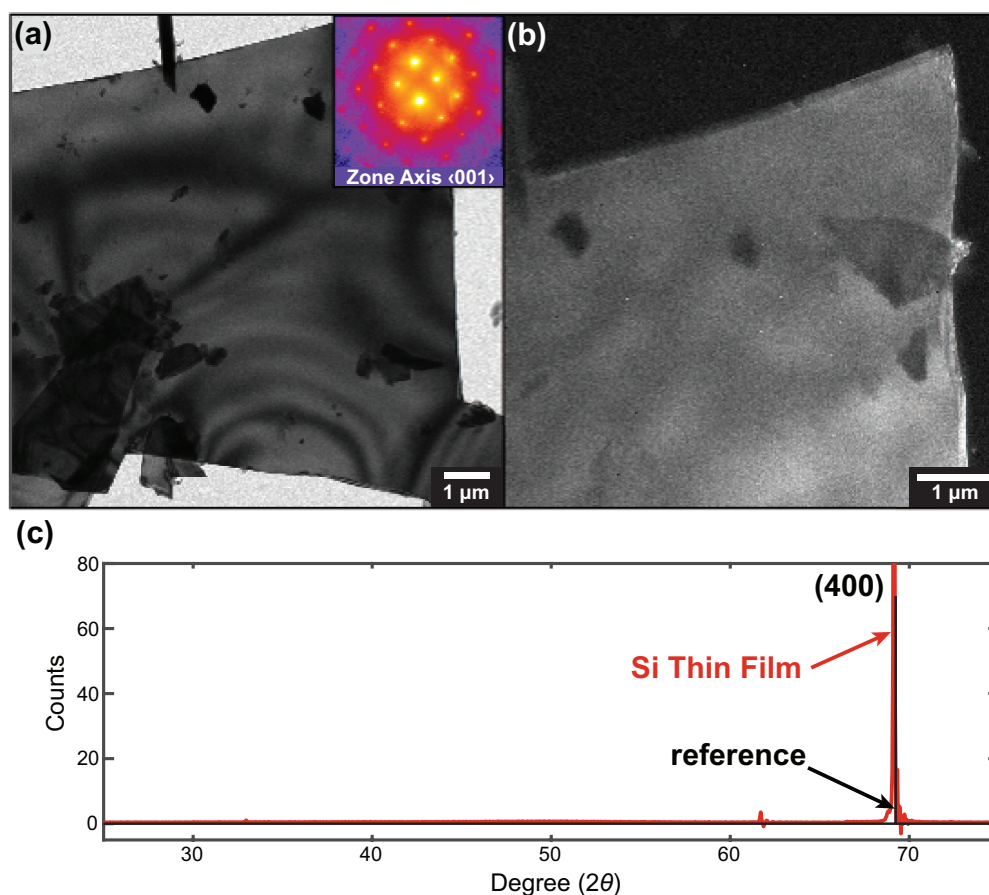


Figure S1: (a) Bright Field TEM image of a flake of the Si thin film sample, with (inset) electron diffraction pattern indicating the $\langle 001 \rangle$ orientation of the entire thin film flake. (b) Dark Field TEM image of the thin film using the (004) diffraction peak shows that the entire membrane flake is a large single crystal domain. (c) X-Ray diffraction of the thin film sample (red) shows only the silicon (400) peak, which is expected for a $\langle 001 \rangle$ oriented crystal. The reference XRD pattern shown is taken from Sun et al. (black).^{S1}

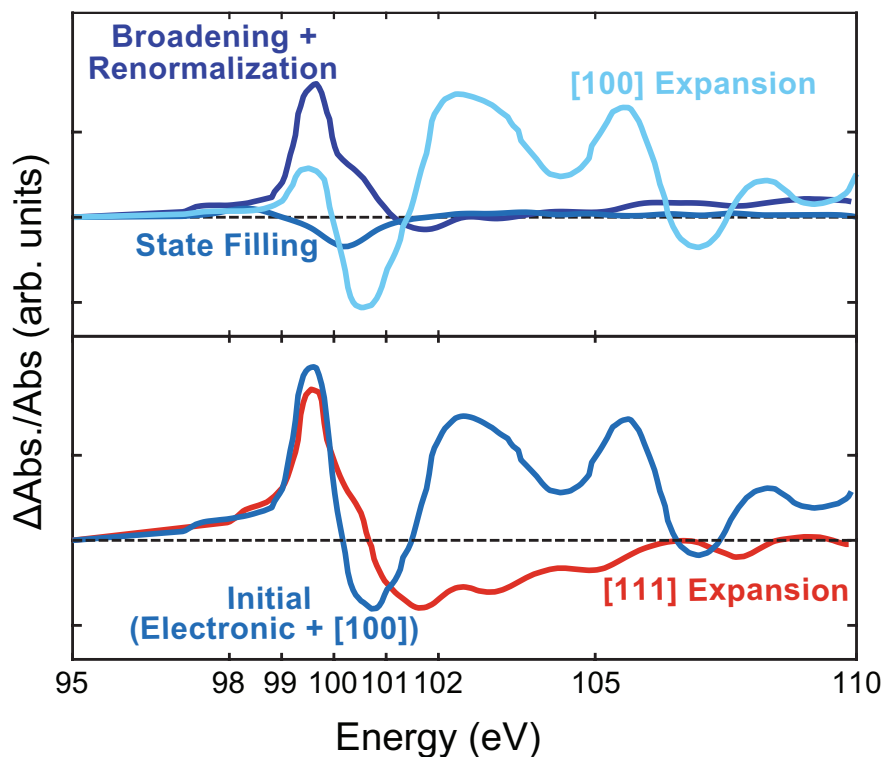


Figure S2: Modeled transient differential spectral signatures of the different components of the thin film Si $L_{2,3}$ edge response, adapted with permission from Cushing, S. K.; Lee, A.; Porter, I. J.; Carneiro, L. M.; Chang, H. T.; Zürich, M.; Leone, S. R. Differentiating photoexcited carrier and phonon dynamics in the Γ , L , and Δ valleys of Si(100) with transient extreme ultraviolet spectroscopy. *J. Phys. Chem. C* **2019**, *123*, 3343-3352. Copyright 2019 Journal of Physical Chemistry C.^{S2} (a) The electronic components of state filling (medium blue) and broadening and renormalization caused by the core hole (dark blue) are shown for a carrier density of $1 \times 10^{19} \text{ cm}^{-3}$. The spectral signature of the optical phonons, modeled as a [100] anisotropic lattice expansion of 5%, is shown in light blue. (b) The sum of the spectral signatures shown in (a) for the electronic and optical phonon components are plotted in blue. The spectral signature of the acoustic phonons, modeled as a [111] isotropic lattice expansion of 5%, is shown in red.

Growth and Decay of circled feature in Figure 3(b) (Corresponding to 1 ps time delay in Figure 3(d))

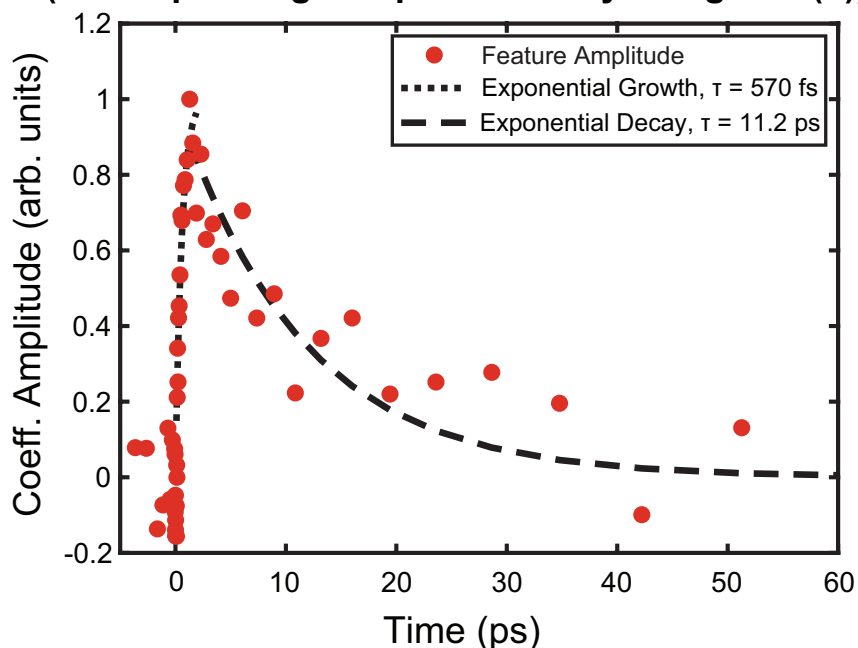


Figure S3: The amplitude of the 1 ps state of a 3-state multivariate regression performed on the nanoparticle sample are shown as red dots for the first 60 ps. The three states used in the regression were the 0.1 ps and 100 ps states, highlighted by dotted lines in Figure 3(b), and the 1 ps state shown in Figure 3(d), middle panel. The uncertainty is indicated by the scatter of the points. The fit using single exponentials of the growth and decay of this state are given by the dotted and dashed lines, respectively. The fits yield a growth time of 570 ± 60 fs and a decay time of 11.2 ± 3.4 ps.

References

- (S1) Sun, Y.; Wu, D.; Liu, K.; Zheng, F. Colossal permittivity and low dielectric loss of thermal oxidation single-crystalline Si wafers. *Materials (Basel)*. **2019**, *12*, 1102.
- (S2) Cushing, S. K.; Lee, A.; Porter, I. J.; Carneiro, L. M.; Chang, H. T.; Zürich, M.; Leone, S. R. Differentiating photoexcited carrier and phonon dynamics in the Δ , L , and Γ valleys of Si(100) with transient extreme ultraviolet spectroscopy. *J. Phys. Chem. C* **2019**, *123*, 3343–3352.